Di-photon Higgs signal at the LHC: a comparative study in different supersymmetric models

Junjie Cao[1], Zhaoxia Heng[1], Tao Liu[2], Jin Min Yang[2]

[1] *Department of Physics, Henan Normal University, Xinxiang 453007, China*

[2] *Key Laboratory of Frontiers in Theoretical Physics,*

Institute of Theoretical Physics, Academia Sinica, Beijing 100190, China

Abstract

As the most important discovery channel for a light Higgs boson at the LHC, the di-photon signal $gg \to h \to \gamma\gamma$ is sensitive to underlying physics. In this work we investigate such a signal in a comparative way by considering three different supersymmetric models, namely the minimal supersymmetric standard model (MSSM), the next-to-minimal supersymmetric standard model (NMSSM) and the nearly minimal supersymmetric standard model (nMSSM). Under the current collider and cosmological constraints we scan over the parameter space and obtain the following observation in the allowed parameter space: (i) In the nMSSM the signal rate is always suppressed; (ii) In the MSSM the signal rate is suppressed in most cases, but in a tiny corner of the parameter space it can be enhanced (maximally by a factor of 2); (iii) In the NMSSM the signal rate can be enhanced or suppressed depending on the parameter space, and the enhancement factor can be as large as 7.

PACS numbers:

I. INTRODUCTION

So far the most important question to be answered in particle physics is the mechanism of the electroweak symmetry breaking and thus hunting for the Higgs boson responsible for it is the main task of current collider experiments. In the framework of the Standard Model (SM), the mass of the Higgs boson is preferred to be $116.4^{+15.6}_{-1.3}$ GeV by precision electroweak data [1]. To search for such a relatively light Higgs boson, great efforts have been made in LEP and Tevatron experiments, which reported null results and excluded a Higgs boson with $m_h \leq 114.4$ GeV [2] and 158 GeV $\leq m_h \leq$ 175 GeV [3] at 95% C.L.. The Large Hadron Collider (LHC) is more powerful in discovering the SM Higgs boson, and depending on its mass, different search strategies will be applied. For a light Higgs boson below 140 GeV, although its largest signal at the LHC is $b\bar{b}$ from the gluon-fusion process $gg \to h \to b\bar{b}$ [4], such a signal is undetectable due to the overwhelming QCD background; instead, the rare decay mode $h \to \gamma\gamma$ with $Br(h \to \gamma\gamma) \simeq 0.2\%$ for m_h =120 GeV offers a very clean signature to make the di-photon signal $gg \to h \to \gamma\gamma$ a promising discovery channel. It is now expected that, with $2fb^{-1}$ integrated luminosity at the LHC running at $\sqrt{s} = 7$ TeV, the di-photon signal is able to exclude the light Higgs boson in the SM [5].

In low energy supersymmetric models (SUSY), the SM-like Higgs boson (the CP-even Higgs boson with largest coupling to gauge bosons) is usually predicted with mass below about 140 GeV. For such a Higgs boson, although there may exist other discovery channels at the LHC, the di-photon channel $gg \to h \to \gamma\gamma$ is still one of the most important discovery modes. So, studying this signal will allow for a probe of low energy SUSY and, as emphasized in [6], even a discrimination of different models. Although in the literature some studies of the signal have been presented in SUSY [7–9], these analyses were performed separately in different models and a comparative study is necessary in order to discriminate the models. In this work we perform such a comparative study by considering three different SUSY models, namely the minimal supersymmetric standard model (MSSM), the next-to-minimal supersymmetric standard model (NMSSM) [10, 11] and the nearly minimal supersymmetric standard model (nMSSM) [12, 13]. We will scan over the parameter space under current constraints from collider experiments and the neutralino dark matter relic density, and then in the allowed parameter space we calculate the di-photon signal rate and compare the results for different models.

This work is organized as follows. We first briefly describe the three supersymmetric models in Sec. II. Then we present our numerical results and discussions in Sec. III. Finally, we draw our conclusions in Sec. IV.

II. SUPERSYMMETRIC MODELS

As the most economical realization of SUSY in particle physics, the MSSM has been intensively studied. However, since this model suffers from the $\mu-$problem and the little hierarchy problem, some of its extensions like the NMSSM and nMSSM were recently paid attention to[10]. The differences of these models come from their superpotentials:

$$W_{\rm MSSM} = W_F + \mu \hat{H}_u \cdot \hat{H}_d, \tag{1}$$

$$W_{\rm NMSSM} = W_F + \lambda \hat{H}_u \cdot \hat{H}_d \hat{S} + \frac{1}{3}\kappa \hat{S}^3, \tag{2}$$

$$W_{\rm nMSSM} = W_F + \lambda \hat{H}_u \cdot \hat{H}_d \hat{S} + \xi_F M_n^2 \hat{S}, \tag{3}$$

where W_F is the MSSM superpotential without the μ term, $\hat{H}_{u,d}$ and $\hat{S}$ are the Higgs doublet and singlet superfields respectively, and the dimensionless coefficients λ, κ and ξ_F and the dimensional coefficients μ and M_n are usually treated as independent parameters. In the NMSSM and nMSSM, when the scalar component (S) of the singlet Higgs superfield $\hat{S}$ develops a vacuum expectation value (VEV), an desired effective μ-term ($\mu_{eff} = \lambda\langle S\rangle$) is generated at the weak scale. Note that the nMSSM differs from the NMSSM in the last term of the superpotential, where the cubic singlet term $\kappa\hat{S}^3$ in the NMSSM is replaced by the tadpole term $\xi_F M_n^2$. Considering that the tadpole term does not induce any interaction, one can infer that, except for the minimization conditions of the Higgs potential and the mass matrices of the Higgs bosons, the nMSSM is actually identical to the NMSSM with vanishing κ.

Corresponding to Eq.(1-3), the soft-breaking terms in Higgs sector are given by

$$V_{\rm soft}^{\rm MSSM} = \tilde{m}_u^2|H_u|^2 + \tilde{m}_d^2|H_d|^2 + (B\mu H_u \cdot H_d + h.c.), \tag{4}$$

$$V_{\rm soft}^{\rm NMSSM} = \tilde{m}_u^2|H_u|^2 + \tilde{m}_d^2|H_d|^2 + \tilde{m}_S^2|S|^2 + (A_\lambda \lambda S H_u \cdot H_d + \frac{A_\kappa}{3}\kappa S^3 + h.c.), \tag{5}$$

$$V_{\rm soft}^{\rm nMSSM} = \tilde{m}_u^2|H_u|^2 + \tilde{m}_d^2|H_d|^2 + \tilde{m}_S^2|S|^2 + (A_\lambda \lambda S H_u \cdot H_d + \xi_S M_n^3 S + h.c.), \tag{6}$$

where $\tilde{m}_u$, $\tilde{m}_d$, $\tilde{m}_S$, B, A_λ and A_κ are all soft parameters. Like the usual treatment of the

multiple Higgs theory, one can write the scalar fields H_u, H_d and S as

$$H_u = \begin{pmatrix} H_u^+ \\ \frac{v_u+\phi_u+i\varphi_u}{\sqrt{2}} \end{pmatrix}, \quad H_d = \begin{pmatrix} \frac{v_d+\phi_d+i\varphi_d}{\sqrt{2}} \\ H_d^- \end{pmatrix}, \quad S = \frac{1}{\sqrt{2}}(s+\sigma+i\xi), \tag{7}$$

and diagonalize the mass matrices of the Higgs bosons to get their mass eigenstates:

$$\begin{pmatrix} h_1 \\ h_2 \\ h_3 \end{pmatrix} = U^H \begin{pmatrix} \phi_u \\ \phi_d \\ \sigma \end{pmatrix}, \quad \begin{pmatrix} a \\ A \\ G^0 \end{pmatrix} = U^A \begin{pmatrix} \varphi_u \\ \varphi_d \\ \xi \end{pmatrix}, \quad \begin{pmatrix} H^+ \\ G^+ \end{pmatrix} = U \begin{pmatrix} H_u^+ \\ H_d^+ \end{pmatrix}. \tag{8}$$

In above expressions, h_1, h_2, h_3 and a, A denote physical CP-even and CP-odd neutral Higgs bosons respectively, G^0 and G^+ are Goldstone bosons eaten by Z and W^+, and H^+ is the charged Higgs boson. Note in the MSSM, due to the absence of S there only exist two CP-even Higgs bosons and one CP-odd Higgs boson, and consequently, U^H and U^A are reduced to 2×2 matrices parameterized by the mixing angles α and β respectively. In our study, we choose the input parameters in the Higgs sector as ($\tan\beta$, m_A, μ) for the MSSM, (λ, κ, $\tan\beta$, μ_{eff}, m_A, A_κ) for the NMSSM with $m_A^2 = \frac{2\mu}{\sin 2\beta}(A_\lambda + \frac{\kappa\mu}{\lambda})$, and ($\lambda$, $\tan\beta$, μ_{eff}, A_λ, $\tilde{m}_S$, m_A) for the nMSSM with $m_A^2 = \frac{2}{\sin 2\beta}(\mu A_\lambda + \lambda\xi_F M_n^2)$.

The Yukawa couplings of the neutral Higgs bosons to the top and bottom quarks are given by [10]

$$\begin{aligned} \mathcal{L}_{\rm Yukawa} &= -\frac{gm_t}{2m_W\sin\beta}U_{i1}^H\bar{t}th_i - \frac{gm_b}{2m_W\cos\beta}U_{i2}^H\bar{b}bh_i \\ &\quad + \frac{igm_t}{2m_W\sin\beta}U_{11}^A\bar{t}\gamma_5 ta + \frac{igm_b}{2m_W\cos\beta}U_{12}^A\bar{b}\gamma_5 ba, \end{aligned} \tag{9}$$

with U^H, U^A defined in Eq.(8). Obviously, once $U_{i2}^H/\cos\beta \ll 1$ as discussed later, the width of $h_i \to b\bar{b}$ is to be suppressed.

Note the properties of the lightest neutralino $\tilde{\chi}_1^0$ in the nMSSM are quite peculiar [13]. After diagonalizing the neutralino mass matrix in the nMSSM, its mass takes the form [14]

$$m_{\tilde{\chi}_1^0} \simeq \frac{2\mu\lambda^2(v_u^2+v_d^2)}{2\mu^2+\lambda^2(v_u^2+v_d^2)}\frac{\tan\beta}{\tan^2\beta+1}, \tag{10}$$

which implies that $\tilde{\chi}_1^0$ must be lighter than about 60 GeV for $\mu > 100$ GeV (required by chargino mass bound) and $\lambda < 0.7$ (required by perturbativity). If $\tilde{\chi}_1^0$ acts as the dark matter candidate, a light CP-odd Higgs boson a is then preferred to accelerate $\tilde{\chi}_1^0$ annihilation to get the acceptable dark matter relic density[13]. Detailed study indicates that $m_{\tilde{\chi}_1^0} \leq 37$ GeV and for most cases, $m_a \leq 60$ GeV, which implies the SM-like Higgs boson h may decay into $\tilde{\chi}_1^0\tilde{\chi}_i^0$ or aa so that $Br(h\to\gamma\gamma)$ is suppressed[13].

III. NUMERICAL RESULTS AND DISCUSSIONS

A. Description of calculations

To compare the signal rate with the SM prediction, we define a normalized rate as

$$\begin{aligned} R^{\rm SUSY} &\equiv \sigma_{SUSY}(pp\to h\to\gamma\gamma)/\sigma_{SM}(pp\to h\to\gamma\gamma) \\ &\simeq [\Gamma(h\to gg)Br(h\to\gamma\gamma)]/[\Gamma(h_{SM}\to gg)Br(h_{SM}\to\gamma\gamma)] \\ &= [\Gamma(h\to gg)\Gamma(h\to\gamma\gamma)]/[\Gamma(h_{SM}\to gg)\Gamma(h_{SM}\to\gamma\gamma)]\times\Gamma_{tot}(h_{SM})/\Gamma_{tot}(h) \end{aligned} \quad (11)$$

where we used the narrow width approximation and the fact that at leading order the cross section of the parton process $gg\to h$ is correlated with the decay width of $h\to gg$ by

$$\hat{\sigma}(gg\to h)=\sigma_0^h m_h^2\delta(\hat{s}-m_h^2)=\frac{\pi^2}{8m_h}\Gamma(h\to gg)\delta(\hat{s}-m_h^2). \quad (12)$$

In SUSY, the $h\gamma\gamma$ coupling arises mainly from the loops mediated by W-boson, charged Higgs boson, charginos and the third generation fermions and sfermions, and the hgg coupling only from the loops mediated by third generation quarks and squarks. Consequently, the widths of $h\to\gamma\gamma, gg$ are given by [7]

$$\Gamma(h\to\gamma\gamma) = \frac{G_F\alpha^2 m_h^3}{128\sqrt{2}\pi}\left|\sum_f N_c\,Q_f^2\,g_{hff}\,A_{1/2}^h(\tau_f)+g_{hWW}\,A_1^h(\tau_W)+\mathcal{A}^{\gamma\gamma}\right|^2, \quad (13)$$

$$\Gamma(h\to gg) = \frac{G_F\alpha_s^2 m_h^3}{36\sqrt{2}\pi^3}\left|\sum_q N_c\,Q_q^2\,g_{hqq}\,A_{1/2}^h(\tau_q)+\mathcal{A}^{gg}\right|^2 \quad (14)$$

where $\tau_i=m_h^2/(4m_i^2)$, and

$$\begin{aligned} \mathcal{A}^{\gamma\gamma} &= g_{hH^+H^-}\frac{m_W^2}{m_{H^\pm}^2}A_0^h(\tau_{H^\pm})+\sum_f N_c Q_f^2 g_{h\tilde{f}\tilde{f}}\frac{m_Z^2}{m_{\tilde{f}}^2}A_0^h(\tau_{\tilde{f}})+\sum_i g_{h\chi_i^+\chi_i^-}\frac{m_W}{m_{\chi_i}}A_{1/2}^h(\tau_{\chi_i}), \\ \mathcal{A}^{gg} &= \sum_i N_c Q_q^2 g_{h\tilde{q}_i\tilde{q}_i}\frac{m_Z^2}{m_{\tilde{q}_i}^2}A_0^h(\tau_{\tilde{q}_i}), \end{aligned} \quad (15)$$

represent pure SUSY contributions with $m_{\tilde{f}}$ and m_{χ_i} being sfermion mass and chargino mass respectively. Noting the asymptotic behavior of A_i^h in the limit $\tau_i\ll 1$[15]

$$A_0^h\to-\frac{1}{3}\,,\quad A_{1/2}^h\to-\frac{4}{3}\,,\quad A_1^h\to+7\,, \quad (16)$$

one can easily learn that the effects of the third generation squarks on the $h\gamma\gamma$ and hgg couplings drop quickly as the squarks becomes heavy, and that the charged Higgs contribution to $h\gamma\gamma$ coupling is usually far smaller than the W-boson contribution.

In SUSY, the third generation squarks can also affect the masses and the couplings of the CP-even Higgs bosons by radiative corrections, and such effects are maximized in the so-called "maximal mixing" (m_h^{max}) scenario defined as $X_t = 2M_{\rm SUSY}$ and $A_t = A_b$ in the on-shell scheme [23], where $X_t = A_t - \mu/\tan\beta$ with A_t denoting the trilinear couplings of the top squarks and M_{SUSY} standing for the common soft breaking mass for the third generation squarks, i.e., $M_{Q_3} = M_{U_3} = M_{D_3} = M_{\rm SUSY}$. Since the corrections are vital for our results, we will specially discuss them later.

Different from previous studies in [6–9], we consider more constraints on the models, which are:

(1) The constraints from the LEP-II direct search for neutral Higgs bosons in various possible channels.

(2) The direct mass bounds on sparticles and Higgs boson from LEP and the Tevatron experiments [16].

(3) The LEP-I constraints on invisible Z decay: $\Gamma(Z \to \tilde{\chi}_1^0\tilde{\chi}_1^0) < 1.76$ MeV, and the LEP-II constraints on neutralino productions $\sigma(e^+e^- \to \tilde{\chi}_1^0\tilde{\chi}_i^0) < 10^{-2}$ pb $(i > 1)$ and $\sigma(e^+e^- \to \tilde{\chi}_i^0\tilde{\chi}_j^0) < 10^{-1}$ pb $(i, j > 1)$ [17].

(4) The indirect constraints from B-physics (such as $b \to s\gamma$) and from the precision electroweak observables such as ρ_ℓ, $\sin^2\theta_{eff}^\ell$ and M_W, or their combinations $\epsilon_i (i = 1, 2, 3)$ [18]. We require ϵ_i to be compatible with the LEP/SLD data at 95% confidence level. We also require new physics prediction of $R_b = \Gamma(Z \to \bar{b}b)/\Gamma(Z \to \text{hadrons})$ is within the 2σ range of its experimental value. The latest results for R_b are $R_b^{exp} = 0.21629 \pm 0.00066$ and $R_b^{SM} = 0.21578$ for $m_t = 173$ GeV [16].

(5) The constraints from Tevatron experiments on $\sigma(p\bar{p} \to h + X \to 4\mu, 2\mu 2\tau)$[19].

(6) The constraints from the muon anomalous magnetic moment: $a_\mu^{exp} - a_\mu^{SM} = (25.5 \pm 8.0) \times 10^{-10}$ [20]. We require the SUSY effects to explain a_μ at 2σ level.

(7) Dark matter constraints from the WMAP relic desity $0.0975 < \Omega h^2 < 0.1213$ [21]. For each model we assume the lightest neutralino as the only component for the dark matter.

As verified by numerous studies, these constraints show strong preference on the SUSY parameters, e.g., the constraint (1) favors heavy top squarks with significant chiral mixing, while the constraint (6) favors large $\tan\beta$ for moderately heavy sleptons. Note that most of the constraints have been encoded in the program NMSSMTools [22], which computes various Higgs decay rates up to one-loop level (the dominant one-loop and leading logarithmic two-loop corrections to the Higgs masses and mixings are also included). We extend the code by adding more constraints in item (4) [24] and further make it applicable to the nMSSM [13] (through some helpful discussions with the authors of the NMSSMTools).

Since the LHC is now testing the probability of the enhanced di-photon signal, we investigate the situation where the signal rate can exceed its SM prediction. Eq.(11) indicates two mechanisms in doing this. One is to enhance the $h\gamma\gamma$ coupling or the hgg coupling. However, as indicated by our numerical results, this mechanism can only enhance the couplings by a factor up to 1.3 and 1.1, respectively. The reason is that the relevant SUSY parameters, such as $\tan\beta$ and the third generation squark masses, have been limited by the constraints. The other mechanism, which proves to be capable in enhancing R^{SUSY} by a factor up to 5, is to suppress the width of $h \to b\bar{b}$ to enhance the branching ratio of $h \to \gamma\gamma$. To understand this, let's look at the expression of $\Gamma(h_i \to b\bar{b})$, which, after including the important SUSY correction to bottom quark mass Δ_b, is given by[25]

$$\Gamma(h_i \to b\bar{b}) \propto \left(\frac{U_{i2}}{\cos\beta}\right)^2 \left(\frac{1 + U_{i1}^H/U_{i2}^H \cot\beta\Delta_b}{1+\Delta_b}\right)^2 \tag{17}$$

where the first factor comes from the bottom Yukawa coupling in Eq.(9) and the second factor arises from transforming the Higgs fields from weak basis to mass eigenstates in the low energy effective Lagrangian. Obviously, once $U_{i2}/\cos\beta \ll 1$ and/or $U_{i1}^H/U_{i2}^H \cot\beta\Delta_b \to -1$, $\Gamma(h_i \to b\bar{b})$ will be greatly suppressed. In the following, we take the MSSM as an example to discuss how to satisfy the conditions.

In the MSSM, Eq.(17) may be rewritten as[23]

$$\Gamma(h \to b\bar{b}) \propto \left(\frac{\sin\alpha}{\cos\beta}\right)^2 \left(\frac{1 - \cot\alpha\cot\beta\Delta_b}{1+\Delta_b}\right)^2 \tag{18}$$

where α is the mixing angle of the two CP-even Higgs boson obtained by diagonalizing the corresponding mass matrix $\mathcal{M}_H^2$, and Δ_b is given by

$$\begin{aligned}\Delta_b &= \Delta_b^{SQCD} + \Delta_b^{SEW} \\ &= \mu\tan\beta\left(\frac{2\alpha_s m_{\tilde{g}}}{3\pi} I(m_{\tilde{b}_1}, m_{\tilde{b}_2}, m_{\tilde{g}}) + \frac{Y_t^2 A_t}{16\pi^2} I(m_{\tilde{t}_1}, m_{\tilde{t}_2}, \mu) + \cdots\right),\end{aligned}$$

with the function I defined by

$$I(a,b,c)=\frac{1}{(a^2-b^2)(b^2-c^2)(a^2-c^2)}\left(a^2b^2\log\frac{a^2}{b^2}+b^2c^2\log\frac{b^2}{c^2}+c^2a^2\log\frac{c^2}{a^2}\right). \quad (19)$$

Given

$$\mathcal{M}_H^2=\begin{pmatrix} m_A^2\sin^2\beta+m_Z^2\cos^2\beta+\Delta_{11} & -(m_A^2+m_Z^2)\sin\beta\cos\beta+\Delta_{12} \\ -(m_A^2+m_Z^2)\sin\beta\cos\beta+\Delta_{12} & m_A^2\cos^2\beta+m_Z^2\sin^2\beta+\Delta_{22}\end{pmatrix}, \quad (20)$$

where Δ_{ij} $(i,j=1,2)$ denote the important radiative corrections with their leading contributions proportional to $\frac{m_t^4}{m_W^2}\ln\frac{m_{\tilde{t}_1}m_{\tilde{t}_2}}{m_t^2}$, one can numerically check that without Δ_{ij}, $\sin\alpha/cos\beta$ is always larger than unity for $\tan\beta>7$ as required by muon anomalous momentum. So to suppress $\sin\alpha$ or equivalently the off-diagonal entry of the mass matrix the radiative correction must be present, and a positive large Δ_{12} along with a light CP-odd Higgs boson is efficiency in doing this. Meanwhile, given $\cot\alpha\cot\beta\sim 1$, Δ_b must be around unity to satisfy $\cot\alpha\cot\beta\Delta_b\to 1$, which requires large $\mu\tan\beta$. In summary, in order to suppress $\Gamma(h_i\to b\bar{b})$, light A as well as large $\mu\tan\beta$ is favored for given sparticle spectrum. We note what we are discussing is actually the so-called 'small $\alpha_{\rm eff}$ scenario' of the MSSM [23].

From Eqs.(11-20) one can infer that, in the heavy sparticle limit, the effective $h\gamma\gamma$ and hgg couplings approach to their SM predictions and R^{SUSY} is determined by $\Gamma(h_i\to b\bar{b})$ or more generally by the total width $\Gamma_{tot}(h)$; while in a general case, the contribution from the sparticle-loops to the couplings may interfere constructively or destructively with its corresponding SM contribution, and the size R^{SUSY} then depends on the competition of $\Gamma(h\to gg)\Gamma(h\to\gamma\gamma)$ with $\Gamma_{tot}(h)$. We checked that this conclusion is also applicable to the NMSSM and the nMSSM.

B. Results for the MSSM in a general scenario

To study R^{SUSY} quantatively we scan over the MSSM parameters under the constraints (1-7) and calculate the di-photon signal rate for the samples surviving the constraints. Since the first two generation squarks have little effects on the di-photon signal rate, in our scan we fix their soft parameters at 1 TeV. As for sleptons, since it only affects significantly the muon anomalous magnetic moment a_μ, which can in turn limit the important parameter $\tan\beta$, we assume all soft parameters in slepton sector to take a common value $m_{\tilde{l}}$ and treat $m_{\tilde{l}}$ as a free parameter. For simplicity, we also assume the grand unification relation for the

gaugino masses, $3M_1/5\alpha_1 = M_2/\alpha_2 = M_3/\alpha_3$ with α_i being the fine structure constants of the different gauge groups. Our scan regions are

$$
\begin{aligned}
&1 \leq \tan\beta \leq 60, \quad 90 \text{ GeV} \leq m_A \leq 1 \text{ TeV}, \\
&200 \text{ GeV} \leq M_{\rm SUSY} (= M_{Q_3} = M_{U_3} = M_{D_3}) \leq 1 \text{ TeV}, \\
&-3 \text{ TeV} \leq A_{t,b} \leq 3 \text{ TeV}, \quad 100 \text{ GeV} \leq \mu, M_2, m_{\tilde{l}} \leq 1 \text{ TeV}.
\end{aligned} \tag{21}
$$

In Fig.1 we display the surviving samples, showing the di-photon signal ratio R^{MSSM} defined in Eq.(11) and the Higgs decay branching ratio versus the mass of the SM-like Higgs boson. This figure shows that in the MSSM there exist some points where R is enhanced by a factor up to 1.5. Such an enhancement is mainly due to the suppression of the total width of h, or equivalently the enhancement of $\mathrm{Br}(h \to \gamma\gamma)$, which is shown in the right frame of Fig.1. Note that we required $\mu < 1$ TeV in our scan. If we relax $\mu < 2$ TeV in the scan, we find that R^{MSSM} can be as large as 4. We checked that those samples giving $R > 1$ actually correspond to the 'small $\alpha_{\rm eff}$ scenario' discussed in [23], which is characterized by a large $\mu \tan\beta$ and $|\sin\alpha_{eff}/\cos\beta| \leq 1$.

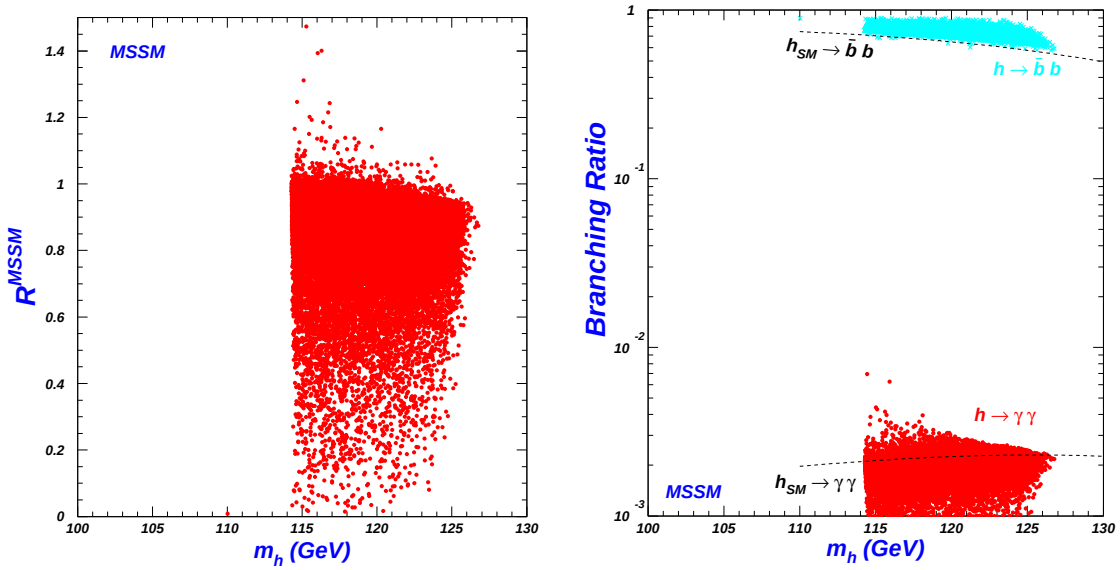

FIG. 1: The scatter plots of the surviving samples, showing the di-photon signal ratio R^{MSSM} defined in Eq.(11) and the Higgs decay branching ratio versus the mass of the SM-like Higgs boson.

Fig.1 also shows that for most of the samples, the rate of the di-photon signal is suppressed relative to its SM prediction. These samples are usually characterized by an enhanced $h\bar{b}b$ coupling and a reduced hgg coupling (the change of the $h\gamma\gamma$ coupling is usually negligible).

We checked that for $R^{SUSY} > 0.6$ the effect of the reduced hgg coupling may be dominant, while for $R^{SUSY} < 0.5$ the effect of the enhanced $h\bar{b}b$ coupling is always dominant. We emphasize that for the samples with $R^{SUSY} < 0.5$, A must be relatively light ($m_A < 300$GeV) to ensure that the properties of h significantly deviate from the SM Higgs boson [26].

We note that current experiments can not rule out a light A with 110 GeV $< m_A <$ 140 GeV in the MSSM [27]. In this case, both A and H (the heavier CP-even Higgs boson) give rise to the di-photon signals similar to the SM-like Higgs boson h. However, the rates of these signals from A and H can not be large. This is because for 110 GeV $< m_A <$ 140 GeV, $\tan\beta$ must be larger than 7 as required by the constraints (particularly by a_μ) [27], which implies $\cos\alpha > 0.8$ from the tree-level relation $\tan 2\alpha = \tan 2\beta \frac{m_A^2+m_Z^2}{m_A^2-m_Z^2}$. Since the $A\bar{b}b$ and $H\bar{b}b$ couplings are proportional to $\tan\beta$ and $\cos\alpha/\cos\beta$ respectively, the branching ratios of $A, H \to \gamma\gamma$ are suppressed and so are their induced di-photon signals at the LHC [28].

C. Results for different models in the m_h^{max} scenario

Since the NMSSM and the nMSSM have more free parameters than the MSSM, it is difficult to perform a general analysis of the signal rate. However, considering our aim is to show the differences of these three models, we examine the signal in the so-called m_h^{max} scenario described in Sec. III A. In this scenario, under the constraints (1-7) we scan over the following parameter ranges:

$$\begin{aligned} &90\ \text{GeV} \le m_A \le 1\ \text{TeV}, 1 \le \tan\beta \le 60,\ 100\ \text{GeV} \le \mu, M_2, m_{\tilde{l}} \le 1\ \text{TeV}, \\ &100\ \text{GeV} \le M_{\text{SUSY}} (= M_{Q_3} = M_{U_3} = M_{D_3}) \le 1\ \text{TeV}, \end{aligned} \tag{22}$$

for the MSSM,

$$\begin{aligned} &0 < \lambda, \kappa \le 0.7,\ 90\ \text{GeV} \le m_A \le 1\ \text{TeV}, \\ &100\ \text{GeV} \le M_{\text{SUSY}} (= M_{Q_3} = M_{U_3} = M_{D_3}) \le 1\ \text{TeV}, \\ &1 \le \tan\beta \le 60,\ |A_\kappa| \le 1\ \text{TeV},\ \ 100\ \text{GeV} \le \mu, M_2, m_{\tilde{l}} \le 1\ \text{TeV}, \end{aligned} \tag{23}$$

for the NMSSM, and

$$\begin{aligned} &0.01 \le \lambda \le 0.7,\ \ 100\ \text{GeV} \le m_A, \mu, M_2 \le 1000\ \text{GeV}, \\ &100\ \text{GeV} \le M_{\text{SUSY}} (= M_{Q_3} = M_{U_3} = M_{D_3}) \le 1\ \text{TeV}, \\ &1 \le \tan\beta \le 60,\ \ -1\ \text{TeV} \le A_\lambda \le 1\ \text{TeV},\ \ 0 \le \tilde{m}_S \le 200\ \text{GeV}, \end{aligned} \tag{24}$$

for the nMSSM with the soft parameters to be 100 GeV for the $(\tilde{\nu}_\mu, \tilde{\mu})$ sector in order to satisfy the a_μ constraint[13]. For other insensitive parameters we adopt the same assumption as in the last section.

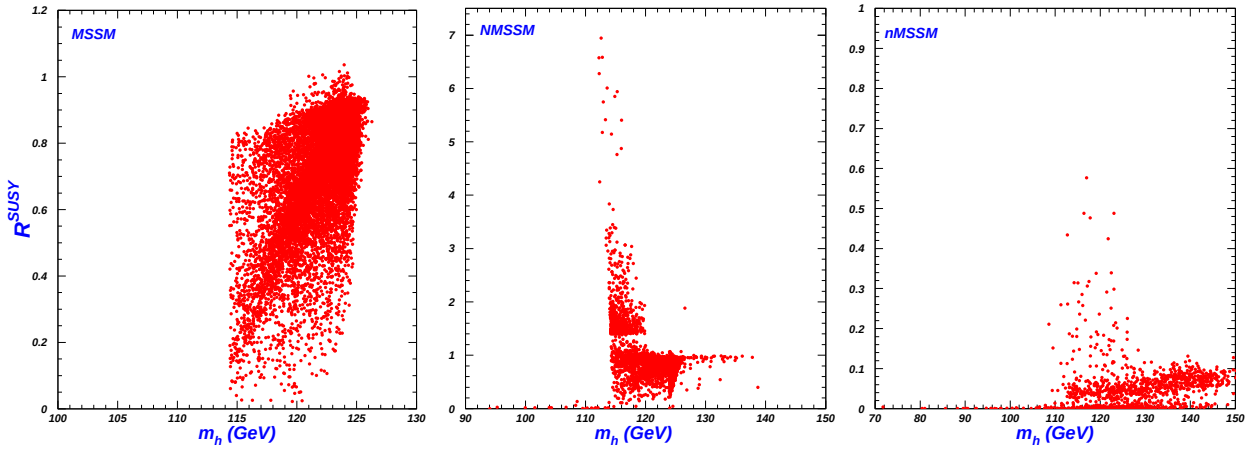

FIG. 2: The scatter plots of the surviving samples in the m_h^{max} scenario of the MSSM, NMSSM and nMSSM, showing the di-photon signal ratio defined in Eq.(11) versus the mass of the SM-like Higgs boson.

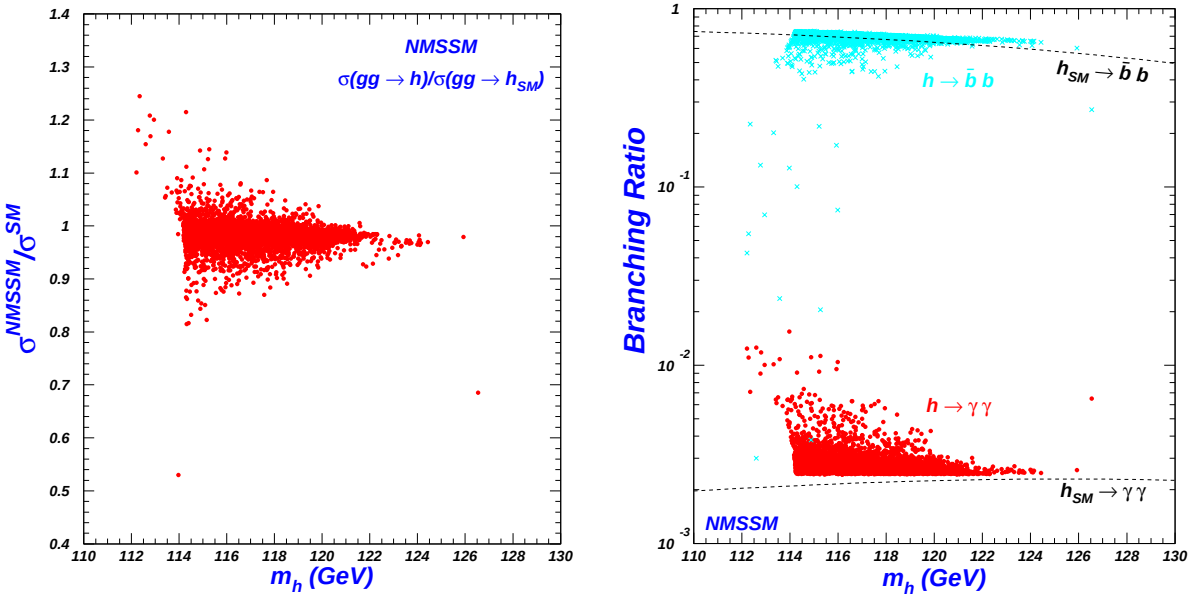

FIG. 3: Same as Fig.2, but projected on different planes for the NMSSM. Here only the samples satisfying $R^{\rm NMSSM} > 1$ are plotted.

In Fig.2 we show the di-photon signal rates in the m_h^{max} scenario for three models. This figure shows that in the nMSSM the signal is always suppressed. In the MSSM the signal is mostly suppressed, but in a tiny part of the parameter space the signal can be slightly

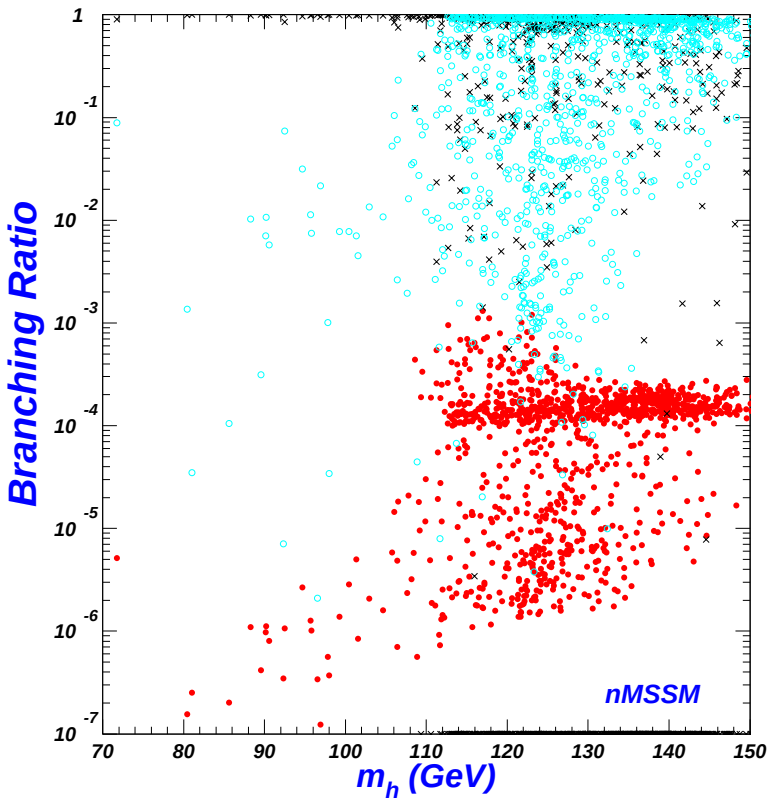

FIG. 4: Same as Fig.2, but showing the branching ratios of the SM-like Higgs decay to $\gamma\gamma$ ('$\bullet$', red), to aa ('$\times$', black), and to $\tilde{\chi}_1^0\tilde{\chi}_1^0$ ('$\circ$', sky blue) in the nMSSM.

enhanced. In the NMSSM, however, the signal can be enhanced in a sizable part of the parameter space (the enhancement factor can be as large as 7). In order to figure out the reason for such a large enhancement in the NMSSM, we concentrate on the samples with $R > 1$ and study the ratio $\sigma^{NMSSM}/\sigma^{SM}(pp \to h)$ and $Br(h \to b\bar{b}, \gamma\gamma)$. Our results are shown in Fig.3, which indicates that the production rate can be enhanced maximally by a factor of 1.25, while $Br(h \to \gamma\gamma)$ can be enhanced to 2×10^{-2} once $Br(h \to b\bar{b})$ is suppressed to several percent. This conclusion justifies our previous analysis about the mechanisms to enhance the signal.

Quite surprisingly, we found that in the NMSSM the samples with $R \gg 1$ are unnecessarily accompanied by a large μ. The fundamental reason is that in SUSY the $h\bar{b}b$ coupling is determined by the H_d component of h, and in the NMSSM, due to the presence of singlet field component in h, the $h\bar{b}b$ coupling can be suppressed more efficiently than in the MSSM. We also noticed that once $Br(h \to b\bar{b})$ is suppressed, $Br(h \to VV^*)$ $(V = W, Z)$ may also get enhanced, which should be limited by the combined search for Higgs boson at

the Tevatron [3]. We checked that for $Br(h \to \gamma\gamma) \sim 10^{-2}$, $Br(h \to VV^*)$ can be enhanced by a factor of 4 relative to its SM prediction.

For the samples with a suppressed di-photon rate in the NMSSM and the nMSSM, we find that $\Gamma_{tot}(h)$ is usually enhanced (due to the enhanced $h\bar{b}b$ and/or the open-up of new decay modes) and the hgg coupling is reduced. We checked that for $R^{SUSY} < 0.5$ the former effect is dominant. We note that in the nMSSM R^{SUSY} is usually small, which is mainly due to the open-up of new decay modes of h, such as $h \to \tilde{\chi}_1^0\tilde{\chi}_i^0$ $(i = 1, 2)$ or $h \to aa$ with their rates shown in Fig.4. We emphasize that this feature comes from the peculiarity of $\tilde{\chi}_1^0$ in the nMSSM (see Eq.(10)) and should keep valid regardless our choice of the soft parameters in the squark sector. We numerically checked this point by a more general scan than Eq.(24). We also note that for nearly all the samples in the NMSSM with $m_h > 120$GeV we have $R^{SUSY} < 1$, and for all the samples in the nMSSM with $m_h > 125$GeV we have $R^{SUSY} < 0.14$. We owe this to the constraints we considered, which severely constrained the enhancement of the branching ratio of $h \to \gamma\gamma$ (see Fig.3 and Fig.4).

We also studied the di-photon signal rate in the 'no-mixing' scenario defined as $A_t = A_b$ and $X_t = 0$. However, we found it is difficult for this scenario to satisfy the constraints if $M_{SUSY} < 1$ TeV, especially we did not find any surviving samples for the MSSM. Since the di-photon signal for the surviving samples in the NMSSM and the nMSSM do not exhibit new characteristics, we do not present the results here.

So, we see that in low energy SUSY, depending on the models, the di-photon signal rate at the LHC may be significantly suppressed or enhanced relative to the SM prediction. With $2fb^{-1}$ integrated luminosity at the running LHC, the di-photon signal can allow for a test of the SM and a probe of the low energy SUSY models. For example, if the di-photon signal rate is found to be not smaller than the SM prediction, then the nMSSM will be immediately excluded (note that in this case the universal extra dimension and the little Higgs theory will also be ruled out because they suppressed the diphoton signal rate [6, 29]).

IV. CONCLUSION

We focused on the di-photon Higgs signal $gg \to h \to \gamma\gamma$ for the SM-like Higgs boson at the LHC and performed a comparative study for three SUSY models: the MSSM, NMSSM and nMSSM. Considering various collider and cosmological constraints, we scanned over the

parameter space and obtained the following observation in the allowed parameter space: (i) In the nMSSM the signal rate is always suppressed; (ii) In the MSSM the signal rate is suppressed in most cases, but in a tiny corner of the parameter space it can be enhanced (maximally by a factor of 2); (iii) In the NMSSM the signal rate can be suppressed or enhanced depending on the parameter space, and the enhancement factor can be as large as 7.

Note added: After we finished the manuscript, we noticed a preliminary result from the ATLAS collaboration [30], which excluded $R \geq 4.2$ (R is defined in Eq.11) for $m_h \simeq 115$GeV. This means that in the middle panel of Fig.2 the samples above $R \simeq 4.2$ for the NMSSM will be excluded.

Acknowledgement

JMY thanks JSPS for the invitation fellowship (S-11028) and the particle physics group of Tohoku University for their hospitality. This work was supported in part by HASTIT under grant No. 2009HASTIT004, by the National Natural Science Foundation of China (NNSFC) under grant Nos. 10821504, 10725526, 10775039, 11075045 and by the Project of Knowledge Innovation Program (PKIP) of Chinese Academy of Sciences under grant No. KJCX2.YW.W10.

[1] M. Goebel (for the Gfitter Group), arXiv:0905.2488.

[2] R. Barate *et al.*, Phys. Lett. B **565**, 61 (2003).

[3] [CDF and D0 Collaboration], arXiv:1007.4587 [hep-ex].

[4] LHC Higgs Cross Section Working Group *et al.*, arXiv:1101.0593 [hep-ph].

[5] I. T. f. Collaboration, arXiv:1012.0694 [hep-ex].

[6] K. Hsieh and C. P. Yuan, Phys. Rev. D **78**, 053006 (2008).

[7] I. Low and S. Shalgar, JHEP **0904**, 091 (2009).

[8] S. Moretti and S. Munir, Eur. Phys. J. C **47**, 791 (2006); U. Ellwanger, arXiv:1012.1201.

[9] M. Almarashi and S. Moretti, arXiv:1011.6547 [hep-ph].

[10] For a review, see, e.g., U. Ellwanger, C. Hugonie and A. M. Teixeira, Phys. Rept. **496**, 1

(2010);

[11] For phenomenological studies, see, e.g., J. R. Ellis *et al.*, Phys. Rev. D **39**, 844 (1989); M. Drees, Int. J. Mod. Phys. A**4**, 3635 (1989); S. F. King, P. L. White, Phys. Rev. D **52**, 4183 (1995); B. Ananthanarayan, P.N. Pandita, Phys. Lett. B **353**, 70 (1995); B. A. Dobrescu, K. T. Matchev, JHEP **0009**, 031 (2000); V. Barger *et al.*, Phys. Rev. D **73**, 115010 (2006); R. Dermisek, J. F. Gunion, Phys. Rev. Lett. **95**, 041801 (2005); G. Hiller, Phys. Rev. D **70**, 034018 (2004); F. Domingo, U. Ellwanger, JHEP **0712**, 090 (2007); Z. Heng *et al.*, Phys. Rev. D **77**, 095012 (2008); R. N. Hodgkinson, A. Pilaftsis, Phys. Rev. D **76**, 015007 (2007); W. Wang *et al.*, Phys. Lett. B **680**, 167 (2009); J. Cao *et al.*, JHEP **0812**, 006 (2008); Phys. Rev. D **78**, 115001 (2008); J. M. Yang, arXiv:1102.4942.

[12] C. Panagiotakopoulos, K. Tamvakis, Phys. Lett. B **446**, 224 (1999); Phys. Lett. B **469**, 145 (1999); C. Panagiotakopoulos, A. Pilaftsis, Phys. Rev. D **63**, 055003 (2001); A. Dedes, *et al.*, Phys. Rev. D **63**, 055009 (2001); A. Menon, *et al.*, Phys. Rev. D **70**, 035005 (2004); V. Barger, *et al.*, Phys. Lett. B **630**, 85 (2005). C. Balazs, *et al.*, JHEP **0706**, 066 (2007).

[13] J. Cao, H. E. Logan and J. M. Yang, Phys. Rev. D **79**, 091701 (2009); J. Cao, Z. Heng and J. M. Yang, JHEP **1011**, 110 (2010).

[14] S. Hesselbach, *et al.*, arXiv:0810.0511v2 [hep-ph].

[15] A. Djouadi, Phys. Lett. B **435**, 101 (1998) [arXiv:hep-ph/9806315].

[16] K. Nakamura *et al.* [Particle Data Group], J. Phys. G **37**, 075021 (2010).

[17] J. Abdallah *et al.*, Eur. Phys. J. C **31**, 421 (2004); G. Abbiendi *et al.*, Eur. Phys. J. C **35**, 1 (2004).

[18] G. Altarelli and R. Barbieri, Phys. Lett. B **253**, 161 (1991); M. E. Peskin, T. Takeuchi, Phys. Rev. D **46**, 381 (1992).

[19] V. M. Abazov *et al.* [D0 Collaboration], Phys. Rev. Lett. **103**, 061801 (2009).

[20] M. Davier *et al.*, Eur. Phys. Jour. C **66**, 1 (2010).

[21] J. Dunkley *et al.* [WMAP Collaboration], Astrophys. J. Suppl. **180**, 306 (2009).

[22] U. Ellwanger, J. F. Gunion and C. Hugonie, JHEP **0502**, 066 (2005); U. Ellwanger and C. Hugonie, Comput. Phys. Commun. **175**, 290 (2006).

[23] M. S. Carena, S. Heinemeyer, C. E. M. Wagner and G. Weiglein, Eur. Phys. J. C **26**, 601 (2003).

[24] J. Cao *et al.*, JHEP **1007**, 044 (2010).

[25] M. S. Carena, D. Garcia, U. Nierste and C. E. M. Wagner, Nucl. Phys. B **577**, 88 (2000).

[26] J. F. Gunion and H. E. Haber, Phys. Rev. D **67**, 075019 (2003).

[27] J. Cao *et al.*, Phys. Rev. D **82**, 051701 (2010).

[28] J. F. Gunion, arXiv:1105.3965 [hep-ph].

[29] L. Wang and J. M. Yang, Phys. Rev. D **79**, 055013 (2009).

[30] The ATLAS collaboration, ATLAS-CONF-2011-085.